MCB
Journals.ASM.org

# Inhibition of Mcl-1 Promotes Senescence in Cancer Cells: Implications for Preventing Tumor Growth and Chemotherapy Resistance

**Elzbieta Bolesta,[d] Lukas W. Pfannenstiel,[b] Abeba Demelash,[b] Mathew L. Lesniewski,[b] Megan Tobin,[b] Simon E. Schlanger,[c] Shreeram C. Nallar,[f] John C. Papadimitriou,[e] Dhan V. Kalvakolanu,[f] and Brian R. Gastman[a,b,d,g]**

Institutes of Head and Neck, Dermatology and Plastic Surgery, Taussig Cancer Center,[a] and Department of Immunology, Lerner Research Institute,[b] Cleveland Clinic, Cleveland, Ohio, USA; Department of Biochemistry, Case Western Reserve University, Cleveland, Ohio, USA[c]; and Departments of Surgery,[d] Pathology,[e] and Microbiology and Immunology[f] and Marlene and Stewart Greenebaum Cancer Center,[g] University of Maryland School of Medicine, Baltimore, Maryland, USA

**Although senescence in oncogenesis has been widely studied, little is known regarding the role of this process in chemotherapy resistance. Thus, from the standpoint of enhancing and improving cancer therapy, a better understanding of the molecular machinery involved in chemotherapy-related senescence is paramount. We show for the first time that Mcl-1, a Bcl-2 family member, plays an important role in preventing chemotherapy-induced senescence (CIS). Overexpression of Mcl-1 in p53$^+$ cell lines inhibits CIS. Conversely, downregulation of Mcl-1 makes cells sensitive to CIS. Surprisingly, downregulation of Mcl-1 in p53$^-$ cells restored CIS to similar levels as p53$^+$ cells. In all cases where senescence can be induced, we observed increased p21 expression. Moreover, we show that the domain of Mcl-1 responsible for its antisenescent effects is distinct from that known to confer its antiapoptotic qualities. *In vivo* we observe that downregulation of Mcl-1 can almost retard tumor growth regardless of p53 status, while overexpression of Mcl-1 in p53$^+$ cells conferred resistance to CIS and promoted tumor outgrowth. In summary, our data reveal that Mcl-1 can inhibit CIS in both a p53-dependent and -independent manner *in vitro* and *in vivo* and that this Mcl-1-mediated inhibition can enhance tumor growth *in vivo*.**

There is growing evidence that senescence is a major barrier in the development of cancer (1, 4). Recently, a network of secreted factors was shown to enforce senescence as a mechanism to prevent tumorigenesis (12, 23). Many of these senescence pathways rely on either p53 or retinoblastoma protein (Rb) tumor suppressors (7). However, data are accumulating on the existence of alternative pathways, which are poorly understood (19). Senescence-like processes also appear to be important forms of cell death induced by both radiation and chemotherapy in cancer (29). Many chemotherapeutics induce the expression of molecules such as p53, which can induce both apoptosis and senescence (16). However, restoring expression of p53 in actively growing cancer prevents tumor progression, not through apoptosis but rather senescence (14, 16). Finally, there is mounting evidence in patients being treated with current anticancer therapies that senescence is often a consequence of treatment (14). Thus, an understanding of the mechanisms of senescence induction in cancer is crucial for designing more effective treatment regimens.

Of the most robust cancer survival molecules are the antiapoptotic members of the Bcl-2 family. Not surprisingly, these proteins can also prevent nonapoptotic cell death pathways such as autophagy and are strongly linked to modulating prosenescent molecules like p53 (1, 11). Furthermore, the senescent state has been linked to being apoptosis resistant through the upregulation of Bcl-2 family members (14). However, their role in modulating senescence is currently poorly understood.

Mcl-1 has a distinct role in the survival and homeostasis of lymphocytes (28). In addition, Mcl-1 appears to be important in the survival of both hematogenous and solid tumors and is now considered a major oncogene (3). For instance, cancer treatment using a small molecule inhibitor capable of preventing the function of Bcl-2 family members but not Mcl-1 fails through a mechanism involving the upregulation of Mcl-1 (22, 33). Whether Mcl-1's survival function includes inhibition of senescence is not known. We therefore hypothesized that Mcl-1 may play an important role in tumor progression through the inhibition of senescence.

Our data show for the first time that Mcl-1 is indeed a major inhibitor of chemotherapy-induced senescence (CIS). Overexpression of Mcl-1 in multiple p53$^+$ tumor and nontumor cell lines was sufficient to block the induction of senescence. Conversely, downregulation of Mcl-1 in p53$^+$ cells resulted in enhanced susceptibility to CIS. We further show that resistance to drug-induced senescence in cells lacking p53 can be overcome by the knockdown of Mcl-1 expression and that this ability to resist senescence in the absence of p53 is unique to Mcl-1 compared to other Bcl-2 family members. We also find that Mcl-1 appears to work downstream of p53 and prevents senescence-associated upregulation of p21 and loss of phosphorylated Rb (pRb) through a mechanism involving reactive oxygen species (ROS) production. Finally, we show that cancer growth and resistance to chemotherapy treatment *in vivo* is highly dependent on the expression of Mcl-1 due in part to the inhibition of senescence and that inhibition of reactive oxygen species (ROS) by an antioxidant can lead to outgrowth of p53$^-$ tumors with low Mcl-1 expression. Successful cancer therapy requires the killing of chemotherapy-resistant tumor cells. Focusing on Mcl-1 from the standpoint of its antisenescence function promises to broaden current anticancer therapeutic regimens.

**Received** 1 September 2011 **Returned for modification** 17 October 2011
**Accepted** 12 March 2012
**Published ahead of print** 26 March 2012
Address correspondence to Brian R. Gastman, gastmab@ccf.org.

doi:10.1128/MCB.06214-11

## MATERIALS AND METHODS

**Cell lines, constructs, and chemotherapies.** The HCT116 human colon cancer cell lines ($p53^+$, $p53^-$, and $p21^-$) were generously provided by Bert Vogelstein (Johns Hopkins University). The HCT116 vector and HCT116 Mcl-1up cell lines were generously provided by Hannah Rabinowich (University of Pittsburgh Cancer Institute). Wild-type murine embryonic fibroblasts (MEFs) were kindly provided by Scott Welford (Case Western Reserve University). $p53^-$ murine embryonic fibroblasts were derived from $p53^-$ C57BL/6 mice as previously described (32). HCT116, HCT116 $p53^-$, HCT116 $p21^-$, HSC-3, MCF-7, MEF, and MEF $p53^-$ were all grown in Dulbecco modified Eagle medium (DMEM) containing penicillin and streptomycin (pen/strep) antibiotics and 10% fetal bovine serum (FBS). MCF-10A and MCF-10A $p53^-$ cells were generously provided by David Weber (University of Maryland School of Medicine) and Ben Ho Park (Johns Hopkins University), respectively. The cells were grown in DMEM containing 50 μg/ml of epidermal growth factor (EGF) from stocks of 100 μg/ml in 10 nM acetic acid, 0.5 μg/ml of hydrocortisone from a 1.0 mg/ml stock dissolved in 95% ethanol, 0.1 μg/ml of cholera toxin, 10 μg/ml human insulin (Sigma, CA), the antibiotics pen/strep, and 5% horse serum (18). All cell cultures were incubated at 37°C in a humidified incubator containing 5% $CO_2$.

HCT116 shControl and HCT116 shMcl-1 cells, HCT116 $p53^-$ shControl, HCT116 $p53^-$ shMcl-1 and HCT116 $p53^-$ shBcl-2 cells, and HCT116 $p21^-$ shControl, and HCT116 $p21^-$ shMcl-1 cells are derivatives of HCT116, HCT116 $p53^-$, and HCT116 $p21^-$ cells, respectively, in which Mcl-1, Bcl-2, and control were stably knocked down using transcript-specific short hairpin RNA (shRNA) expression vectors (Open Biosystems). Sequences that target Mcl-1 are as follows: shMcl-1 cl.1, GAAATTCTTTCACTTCATT; shMcl-1 cl.2, GCTTGTAAATGTATTTGTA; shMcl-1 cl.3, AGGATTATGGCTAACAAGA. Sequences that target Bcl-2 are as follows: shBcl-2 cl.1, CCCTGATTGTGTATATTCA; shBcl-2 cl.2, CGAAGAACCTTGTGTGACA; shBcl-2 cl.3, CCTTGAAACATTGATGGAA; shBcl-2 cl.4, CTTGGACAATCATGAAATA. The Mcl-1 BH3 binding domain mutant was generously provided by Hannah Rabinowich (University of Pittsburgh School of Medicine), identical to the one described in Clohessy et al. (13). The Mcl-1ΔC mutant was generously provided by Douglas Green (St. Jude's Hospital) in the pET plasmid (10), from which the open reading frame (ORF) was PCR cloned into the pCR4.1 His-tagged mammalian expression vector purchased from Invitrogen. Doxorubicin (Sigma) was used *in vitro* at 100 ng/ml and *in vivo* at 1.2 mg/kg. Paclitaxel (Cell Signaling) was used at 10 μM to induce senescence in MEF and MEF $p53^-$. TW37 (2 nM) was a gift from Shaomeng Wang (University of Michigan, Ann Arbor, MI), ABT737 (10 μM) was provided by Abbott Laboratories (Abbott Park, IL), and AT101 (2.5 μM) and roscovitine (25 μM) (Sigma) were used in the indicated experiments.

**Transient transfections.** Transient plasmid transfection into different cell lines was performed by Lipofectamine 2000 (Invitrogen) according to the manufacturer's instructions. Briefly, cells ($2.5 \times 10^5$ per well) were seeded into 6-well plates and transfected with 0.5 μg of an Mcl-1 BH3 binding groove mutant, Mcl-1ΔC mutant, Bcl-2, or Bcl-xL expressing construct or the empty vector. Transient control and Bcl-xL small interfering RNA (siRNA) transfections were also performed using Lipofectamine 2000 (Invitrogen) according to the manufacturer's instructions. Medium was changed after 24 h. Cells were incubated at 37°C in a 5% $CO_2$ incubator for 48 h prior to testing for transgene expression or knockdown by Western blotting.

**Western blotting.** Western blot analyses were performed as described previously (28). In brief, total protein from cell lysates (30 to 50 μg) was loaded for each sample lane. Proteins were separated by SDS-PAGE and transferred to a nitrocellulose or polyvinylidene fluoride membrane (Bio-Rad Laboratories, Hercules, CA). Western blots were developed using the enhanced chemiluminescence (ECL) reagents (GE Healthcare). Primary antibodies used for Western blotting were anti-Mcl-1, anti-p53 (Santa Cruz Biotechnology), anti-p21, anti-pRb (S807/811), anti-Rb (Cell Signaling Technology), anti-Bcl-2 (BD Pharmigen), and anti-β-actin (Sigma). Horseradish peroxidase (HRP)-linked secondary antibodies were purchased from Cell Signaling Technology. Comparable protein loading was ensured by reprobing the blots with a mouse anti-β-actin monoclonal antibody.

**Quantitative *in situ* SA-β-gal assay.** Cells were seeded into 6-well plates in a DMEM culture medium, and after 24 h, 100 ng/ml doxorubicin was added. The cells were then incubated for 3 to 6 days. SA-β-$gal^+$ staining was followed by the manufacturer's protocol (Cell Signaling Technology). Several representative fields ($n = 20$) were randomly selected for the quantification of the percentage of SA-β-$gal^+$ cells. Frozen tumor sections were fixed and stained for SA-β-gal activity using X-Gal (5-bromo-4-chloro-3-indolyl-β-D-galactoside) at pH 6.0, following the protocol recommended by the manufacturer (Cell Signaling Technology).

**Quantitative PML body immunohistological staining.** Cell lines were plated at $1.0 \times 10\wedge 5$ to $2.0 \times 10^5$ cells per well in each well of a 6-well plate containing a poly-L-lysine-treated coverslip. Plates were then incubated overnight in 3 ml of medium to allow cells to adhere. The next day, the chemotherapeutic agent was added to half the samples. Treated cells were left to incubate for 96 h, at which time the cells were fixed with ice-cold methanol and then washed in phosphate-buffered saline (PBS). The cells were permeabilized by incubation in PBS containing 0.25% Triton X-100 (PBS-T) for 10 min, followed by 3 washes in PBS. The fixed cells were then placed in a blocking buffer containing PBS-T and 1% bovine serum albumin (BSA) for 30 min. Next, coverslips were incubated in the above-described blocking buffer containing a 1:200 dilution of mouse monoclonal antibody to PML nuclear bodies (Santa Cruz Biotechnology, Santa Cruz, CA) for 1 h. The coverslips were washed three times in PBS-T and then incubated for 1 h in the dark with a goat anti-mouse secondary antibody conjugated with Cy3 (Biolegends, CA). The coverslips were then washed three times with PBS-T and mounted on microscope slides using Vectashield mounting medium containing DAPI (4′,6-diamidino-2-phenylindole) for fluorescence (Vector Laboratories, Burlingame, CA). The slides were then observed using a mercury arc lamp and both Texas Red and DAPI filters. Images were merged using Qcapture software suite. The number of PML nuclear bodies per nucleus was determined using a Leica DM5500 B florescent microscope at both 40× and 100× oil immersion. Multiple experiments were incorporated into the figures, and at least 30 nuclei from random fields were selected to obtain the number of PML bodies.

**Determination of ROS production.** Cells were grown in 6-well plates for 2 days and then left untreated or treated with 5 μM the antioxidant *N*-acetyl-L-cysteine (NAC) (Sigma-Aldrich) for 24 h. The cells were then treated with 100 ng/ml doxorubicin or left untreated for 6 days as indicated. ROS production was detected using a cell-permeable fluorescent molecule, RedoxSensor Red CC-1 (R-14060; Molecular Probes), in phenol-red-free medium as described in the manufacturer's protocol. The involvement of ROS production in p21 activation was determined by Western blotting after 6 days of doxorubicin treatment. β-Actin was used as an internal control.

**Clonogenic assay (colony escape assay).** Cells were plated at a known cell density and exposed to doxorubicin at 100 ng/ml the next day. Colonies typically emerged 14 to 21 days following chemotherapy and are scored from triplicate plates. Colonies were fixed with methanol and stained with 0.1% crystal violet in 20% methanol for 15 min. Colony numbers were determined by manual counting.

**BrdU incorporation assay.** Cells were treated overnight with BrdU and the extent of BrdU incorporation was assayed using the APC BrdU flow kit (BD Pharmingen), followed by flow cytometric analysis. BrdU flow data were tabulated and analyzed using FlowJo (Tree Star, Inc., Ashland, OR).

***In vivo* tumor growth.** Female athymic NCr-nu/nu mice (6 weeks old) were obtained from the National Cancer Institute (NCI). HCT116 shControl, HCT116 shMcl-1, HCT116 vector, HCT116 Mcl-1up, HCT116 $p53^-$ shControl, and HCT116 $p53^-$ shMcl-1 tumor cells were

injected subcutaneously (s.c.) at the right dorsal flank of recipient mice ($1 \times 10^7$ cells per mouse). Doxorubicin (Sigma) at 1.2 mg/kg suspended in PBS (pH 7) was administered intraperitoneally every third day, starting at day 10, after transplantation of tumor cells. Control animals bearing s.c. flank tumors were treated with PBS. Antioxidant-treated mice received drinking water supplemented with 40 mM *N*-acetylcysteine (NAC; Sigma) to yield an average dose of 1 g NAC per kg body weight per day (27). NAC-treated water was replaced every third day. The length ($L$) and width ($W$) of the tumor were measured with calipers every third day, and the tumor volume (TV) was calculated as $TV = (L \times W^2)/2$. All animals were maintained in pathogen-free animal facilities at the University of Maryland School of Medicine and Cleveland Clinic Lerner Research Institute, and all procedures were performed under respective institutional animal care and use committee approved protocols.

**Immunohistochemical analysis.** Tumor tissues from mice were fixed overnight in cold 4% paraformaldehyde (prepared in PBS) at 4°C, followed by incubation in cold 30% sucrose/PBS solution for 24 h before embedding in optimal cutting temperature (OCT) medium (Tissue-Tek; Sakura) on dry ice and stored at −70°C. Tissue sections (7 μm thick) were mounted on gelatin-coated slides and then stored at −70°C. Immunofluorescence and immunohistochemical staining for Mcl-1 and Ki-67 was performed as described elsewhere (10, 30). Terminal deoxynucleotidyltransferase-mediated dUTP-biotin nick end labeling (TUNEL) staining was performed using the ApopTag kit using the manufacturer's protocol (Millipore) and compared to a commercially prepared positive-control slide (Millipore).

**Statistical analysis.** Data are presented as mean ± standard deviation (SD) or mean ± standard error of the mean (SEM) from at least three separate experiments. Differences between various experimental groups were calculated using Student's $t$ test, in which $P$ values of $<0.05$ were considered significant. The Mann-Whitney nonparametric test established the significance for the change in the number of PML bodies with a $P$ value of $<0.05$ considered significant.

## RESULTS

**Mcl-1 inhibits CIS in multiple cell types.** Mcl-1 is frequently overexpressed in neoplastic tissues and can confer resistance to cancer therapies (31, 40). We first sought to determine if Mcl-1 confers resistance to CIS in cancer by utilizing a well-characterized model of HCT116 colon carcinoma cells expressing an intact copy of p53 but with an inactive *INK4A* locus that impairs the expression of p16 and $p14^{ARF}$ (26). Previous studies have reported that a low dose of doxorubicin induces senescence in these cells (17). We therefore exposed derivatives of this cell line (37), either overexpressing Mcl-1 (HCT116 Mcl-1up) or an empty vector (HCT116 vector), to a low dose of doxorubicin (100 ng/ml) for 6 days. The level of Mcl-1 expression in these lines was verified by Western blot analysis (Fig. 1A). As expected, HCT116 vector cells treated with doxorubicin adopted a senescent phenotype typified by a large, flattened shape and enhanced expression of SA-β-galactosidase (SA-β-$gal^+$) in about 60% of cells (Fig. 1A and B). Although SA-β-gal is the most common assay used to analyze senescence, others have shown that the formation of PML bodies within the nuclei along with SA-β-$gal^+$ is confirmatory of senescence (28). Our data are consistent, as control cells induced to senesce have significant increases in the number of nuclear PML bodies compared to untreated cells. However, cells overexpressing Mcl-1 had significant abrogation of senescent changes after treatment, including reduced SA-β-$gal^+$ and no increase in PML foci compared to HCT116 empty vector cells (Fig. 1A and B).

To confirm our results, we overexpressed Mcl-1 in other $p53^+$ cell lines: MCF-7 (breast) and MEL526 (melanoma). Both were transiently transfected using either empty vector or one overexpressing Mcl-1. The cells were allowed to rest for 48 h and were then treated with 100 ng/ml of doxorubicin for 6 days. MCF-7 and MEL526 cell lines showed statistically significant reductions in the percentage of SA-β-$gal^+$ cells in the Mcl-1 overexpressing cell lines treated with doxorubicin compared to respective vector controls (Fig. 1C).

We next employed two noncancer cell lines: MCF-10A (immortalized breast epithelium) and mouse embryonic fibroblasts (MEFs) (31, 32). Both were transiently transfected with either the empty or Mcl-1 overexpressing vector. In the case of MCF-10A, after 48 h, cells were exposed to 100 ng/ml of doxorubicin for 6 days. MCF-10A cells containing the empty vector exhibited a senescent morphology when treated with low-dose chemotherapy, while those overexpressing Mcl-1 had a significant reduction in SA-β-$gal^+$ cells compared to control (Fig. 1C). Finally, we examined chemotherapy-induced senescence in primary cells (MEFs). Initially, we attempted to use doxorubicin but found that paclitaxel yielded the most robust induction of senescence. Similar to the previous cell lines described, MEFs overexpressing human Mcl-1 were relatively resistant to CIS (Fig. 1C). Human Mcl-1 similarly has been described to inhibit apoptosis in mice, thus the survival functions of Mcl-1 do not appear to be limited to species from which it was derived (40). Thus, overexpression of Mcl-1 in $p53^+$ cells is sufficient to protect from CIS regardless of cell origin.

In addition to measuring SA-β-$gal^+$ cells and PML bodies to identify senescence, we obtained supporting evidence for the senescent phenotype using a clonogenic escape assay and BrdU incorporation (Fig. 1D and E). In the clonogenic assay, the number of untreated control and Mcl-1 overexpressing colonies was comparable on day 15 of the experiment. In contrast, doxorubicin-treated control cells formed significantly fewer colonies compared to those overexpressing Mcl-1. In addition, using the BrdU incorporation assay, we observe that the proliferation of cells growing in drug-free media was equivalent regardless of the level of Mcl-1 expression and that doxorubicin treatment of control cells resulted in a marked decrease in BrdU incorporation. However, overexpression of Mcl-1 resulted in only a slight decline in BrdU uptake after drug treatment. These results further confirm our observation that doxorubicin treatment reduced the proliferation of control cells but had little effect on those overexpressing Mcl-1.

We next examined whether the addition of low-dose chemotherapy alters Mcl-1 protein levels either in control or in Mcl-1 overexpressing HCT116 cells. Though we have found Mcl-1 expression to decrease slightly and then rebound over the first 24 h of drug treatment (data not shown), we find that Mcl-1 protein levels are not significantly affected by longer-term culture in doxorubicin for up to 6 days (Fig. 1F). The lack of significant loss of Mcl-1 during CIS is in stark contrast to what has been reported to occur during chemotherapy-induced apoptosis, which further distinguishes senescence from this form of cell death (17).

To understand the role of Mcl-1 in the inhibition of CIS, we evaluated the expression of some of the key molecules known to be involved in cellular senescence: p53, p21, Rb, and pRb (S708/711, pRb). We noticed that the accumulation of p53 in cells overexpressing Mcl-1 and treated with doxorubicin is the same as in control cells despite a significant difference in SA-β-gal-activity. However, in contrast to controls, Mcl-1 overexpressing cells had a lower accumulation of p21 and an increased (versus loss in controls) accumulation of Rb and pRb. These data suggest that Mcl-1 inhibits CIS downstream or at the level of p53

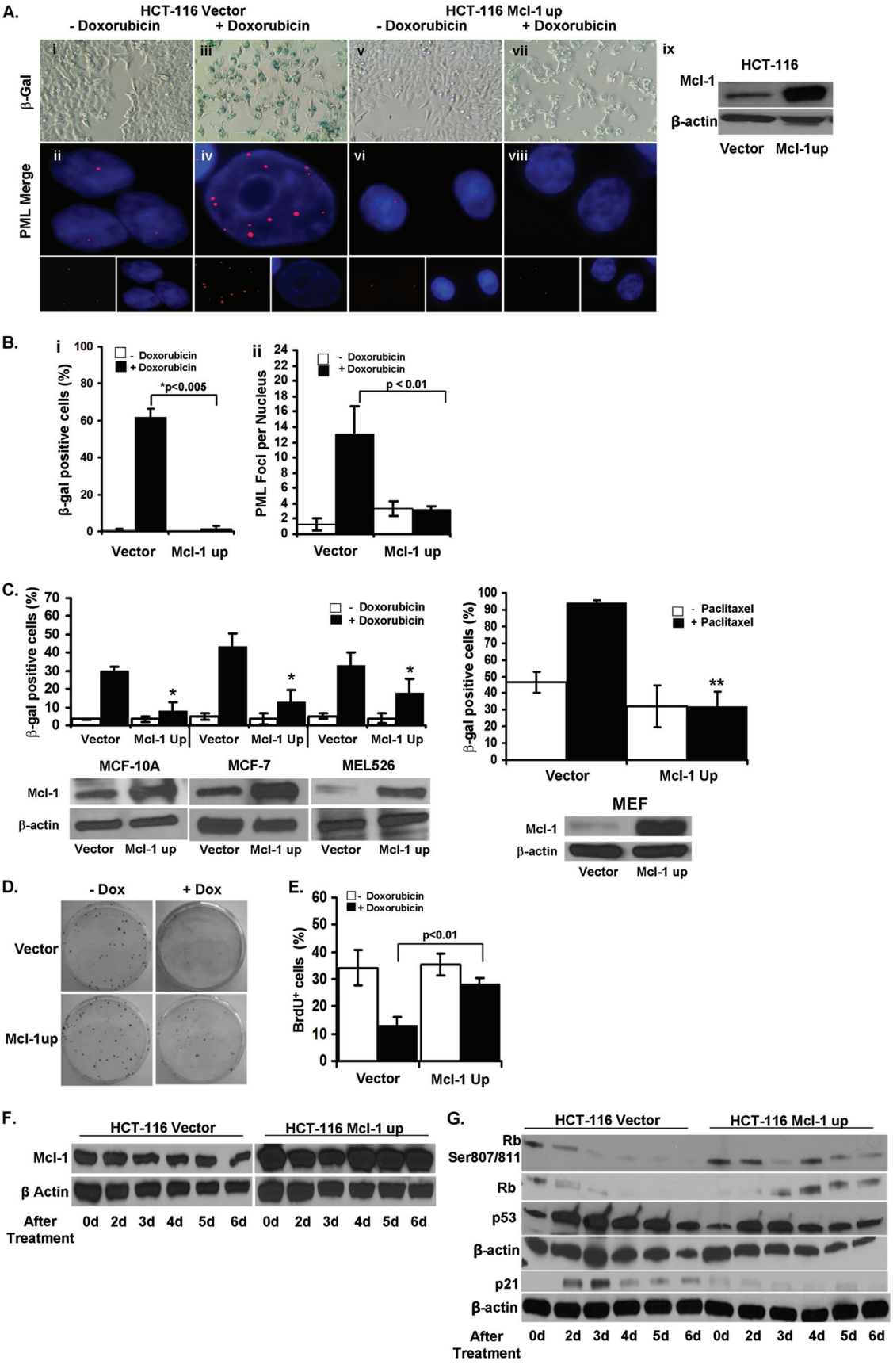
A.
HCT-116 Vector
- Doxorubicin
+ Doxorubicin
HCT-116 Mcl-1 up
- Doxorubicin
+ Doxorubicin
β-Gal
PML Merge
i
ii
iii
iv
v
vi
vii
viii
ix
HCT-116
Mcl-1
β-actin
Vector
Mcl-1up
B.
i
β-gal positive cells (%)
- Doxorubicin
+ Doxorubicin
*p<0.005
Vector
Mcl-1 up
ii
PML Foci per Nucleus
- Doxorubicin
+ Doxorubicin
p < 0.01
Vector
Mcl-1 up
C.
β-gal positive cells (%)
- Doxorubicin
+ Doxorubicin
Vector
Mcl-1 Up
MCF-10A
MCF-7
MEL526
Mcl-1
β-actin
Vector
Mcl-1 up
β-gal positive cells (%)
- Paclitaxel
+ Paclitaxel
**
Vector
Mcl-1 Up
MEF
Mcl-1
β-actin
Vector
Mcl-1 up
D.
- Dox
+ Dox
Vector
Mcl-1up
E.
BrdU+ cells (%)
- Doxorubicin
+ Doxorubicin
p<0.01
Vector
Mcl-1 Up
F.
HCT-116 Vector
HCT-116 Mcl-1 up
Mcl-1
β Actin
After Treatment
0d 2d 3d 4d 5d 6d 0d 2d 3d 4d 5d 6d
G.
HCT-116 Vector
HCT-116 Mcl-1 up
Rb Ser807/811
Rb
p53
β-actin
p21
β-actin
After Treatment
0d 2d 3d 4d 5d 6d 0d 2d 3d 4d 5d 6d

and subsequently blocks the accumulation of p21 and loss of pRb (Fig. 1G).

To determine if CIS alters the binding of Mcl-1 to p53, we used coimmunoprecipitation (co-IP) to assess whether there are changes in their binding relationship, as we previously described during apoptosis (18). We observed that low-dose doxorubicin treatment did not alter the binding relationship between p53 and Mcl-1 in cells overexpressing Mcl-1, further distinguishing CIS from changes observed during apoptosis (data not shown).

**Downregulation of Mcl-1 augments CIS in HCT116 cells.** We next examined if downregulation of Mcl-1 could enhance CIS. We generated a number of HCT116 cell lines stably expressing a Mcl-1-specific short hairpin RNA (shRNA) or an irrelevant control. After verifying the knockdown of Mcl-1 (Fig. 2A), cells were then treated with doxorubicin and analyzed 6 days later for SA-β-gal activity. In all treated cell lines, we observed typical increases in SA-β-gal$^+$ cells (Fig. 2A). However, significantly higher percentages of SA-β-gal$^+$ cells, as well as higher numbers of PML bodies, were observed in doxorubicin-treated shMcl-1-expressing cells compared to controls (Fig. 2A and B). Additionally, Mcl-1 downregulation alone did not significantly affect cell proliferation in clonogenic or BrdU uptake assays, even after low-dose doxorubicin treatment (Fig. 2C and D). We further examined the effect long-term doxorubicin treatment had on control and shMcl-1 cells. Similar to our previous findings, doxorubicin treatment had a minimal effect on Mcl-1 levels in control cells, while a noticeable reduction in Mcl-1 expression was found in shMcl-1 cells over the first 3 days of treatment (Fig. 2E). Though Mcl-1 levels returned in these cells by day 4, the expression continued to be reduced compared to those expressing the control vector. Further, despite the increase in SA-β-gal activity in drug-treated shMcl-1 cells, there was no difference in p53, p21, Rb, or pRb expression in comparison to shControl cells undergoing senescence (Fig. 2F). These data indicate that base levels of Mcl-1 at least partially prevent senescence induction in response to DNA damage in HCT116 cells.

**Downregulation of Mcl-1 allows for CIS in HCT116 p53$^-$ cells.** Many tumors have inactive p53, which results in resistance to both apoptosis and senescence (5, 34). Our data show that overexpression of Mcl-1 in p53$^+$ cells inhibits CIS while downregulation can enhance it. Therefore, we wanted to know if downregulation of Mcl-1 in p53$^-$ cells also sensitizes them to CIS. We stably transfected a previously developed HCT116 p53$^-$ cell line with either control plasmid or shMcl-1 and generated a number of clones (6). After verifying the downregulation of Mcl-1 by Western blotting (Fig. 3A), these cells were treated with doxorubicin and analyzed 6 days later. As expected, HCT116 p53$^-$ shControl cells treated with doxorubicin did not show any senescent phenotypic changes, did not lose expression of Mcl-1, had no detectable SA-β-gal activity, and few PML bodies (Fig. 3A and B). In contrast, each HCT116 p53$^-$ shMcl-1 clone adopted a senescent phenotype and had increased SA-β-gal activity and PML staining, similar to their p53$^+$ counterparts (Fig. 3A and B). We also observe induction of SA-β-gal activity after knockdown of Mcl-1 in other p53$^-$ cell lines, namely, HSC3 and p53$^-$ MEFs (Fig. 3D). In addition, we obtained the recently derived MCF-10A immortalized human mammary cell line possessing a somatic deletion of p53. MCF-10A p53$^-$ cells have a significantly increased sensitivity to DNA-damaging chemotherapies (35); however, their sensitivity to CIS has not been reported. Unlike HCT116 p53$^-$ cells, doxorubicin treatment of MCF-10A p53$^-$ cells resulted in a significant increase in the percentage of SA-β-gal$^+$ cells compared to untreated controls (Fig. 3D). This result required a change in our strategy, and we instead overexpressed Mcl-1 to see if enhanced Mcl-1 expression could resist the induction of CIS. Indeed, we did observe a loss of senescence in these cells (Fig. 3D). Thus, Mcl-1 appears to have a significant antisenescent role in cells lacking p53.

Consistent with the increased SA-β-gal$^+$ activity and PML body formation in response to low-dose chemotherapy, HCT116 p53$^-$ shMcl-1 cells lost the ability to form colonies (Fig. 3E) and proliferated at a level lower than that observed with treated HCT116 p53$^-$ shControl cells (Fig. 3F). To further understand this p53-independent pathway of senescence, we evaluated the expression of p21 and pRb in HCT116 p53$^-$ shMcl-1 cells and HCT116 p53$^-$ shControl cells in the presence of doxorubicin (Fig. 3G). Cells expressing lower levels of Mcl-1 and treated with doxorubicin had greater p21 expression than the corresponding control cells. Furthermore, pRb and levels of total Rb were suppressed in HCT116 p53$^-$ shMcl-1 cells versus controls. These data suggest that Mcl-1 blocks CIS in p53$^-$ cell lines and that by depleting Mcl-1, senescence is restored via a concomitant induction of p21 and a reduction of pRb.

To further validate the role of Mcl-1 in the induction of senescence in the p53$^-$ cells, we employed a cyclin-dependent kinase (CDK) inhibitor (roscovitine) to block Mcl-1 activity. Data from several laboratories has established that CDK inhibitors act, at least in part, by inhibiting CDK9, a kinase intimately involved in transcription initiation and elongation factor b, resulting in downregulation of several short-lived proteins, including Mcl-1 (9). Similar to HCT116 p53$^-$ shMcl-1 cells, roscovitine (25 μM) and low-dose doxorubicin treatment of HCT116 p53$^-$ cells re-

**FIG 1** Overexpression of Mcl-1 in HCT116 cells abrogates CIS. (A) SA-β-gal staining of HCT116 vector and Mcl-1up cells grown with or without 100 ng/ml doxorubicin (Dox) for 6 days (panels i, iii, v, vii) (magnification, ×100). HCT116 vector and Mcl-1up cells grown with or without doxorubicin for 4 days, followed by staining with anti-PML antibody and secondary antibody conjugated to Cy3 (red) and nuclei counterstained with DAPI (panels ii, iv, vi, viii) (magnification, ×100). Western blot verifying overexpression of Mcl-1. (B) Percentages of SA-β-gal+ cells among HCT116 vector and Mcl-1up cells after 6 days with and without doxorubicin (panel i). Values represent the mean and standard error of the mean (SEM) of at least 3 independent experiments. PML bodies per nucleus in HCT116 vector and Mcl-1up cells after 4 days with or without doxorubicin (panel ii). Values represent the mean and SEM of at least three independent experiments. **, *P* value of <0.05 between treated and untreated HCT116 vector cells using a Mann-Whitney statistical test. (C) Percentages of SA-β-gal+ cells among MCF-10A, MCF-7, MEL526, and mouse embryonic fibroblast (MEF) cells transformed with either vector or Mcl-1up after 6 days treated with and without doxorubicin or 10 μM paclitaxel in the case of the MEFs. Values represent the mean ±SEM of at least three independent experiments. *, *P* value of <0.01 compared to doxorubicin-treated vector control cells of each type. **, *P* value of <0.001 between doxorubicin-treated vector and Mcl-1up MEF cells. Western blots verifying overexpression of Mcl-1 in the indicated cell lines. (D) Colony formation by HCT116 vector and Mcl-1up cells growing with or without doxorubicin. (E) Quantification of BrdU incorporation by HCT116 vector and Mcl-1up cells. Values represent the mean and standard deviation (SD) of at least 3 independent experiments. (F) Mcl-1 expression in HCT116 cells was verified by Western blotting at the indicated time points after treatment with 100 ng/ml doxorubicin. (G) Western blot analysis of indicated protein expression in untreated cells (0 days) and 2, 3, 4, 5, and 6 days following doxorubicin treatment.

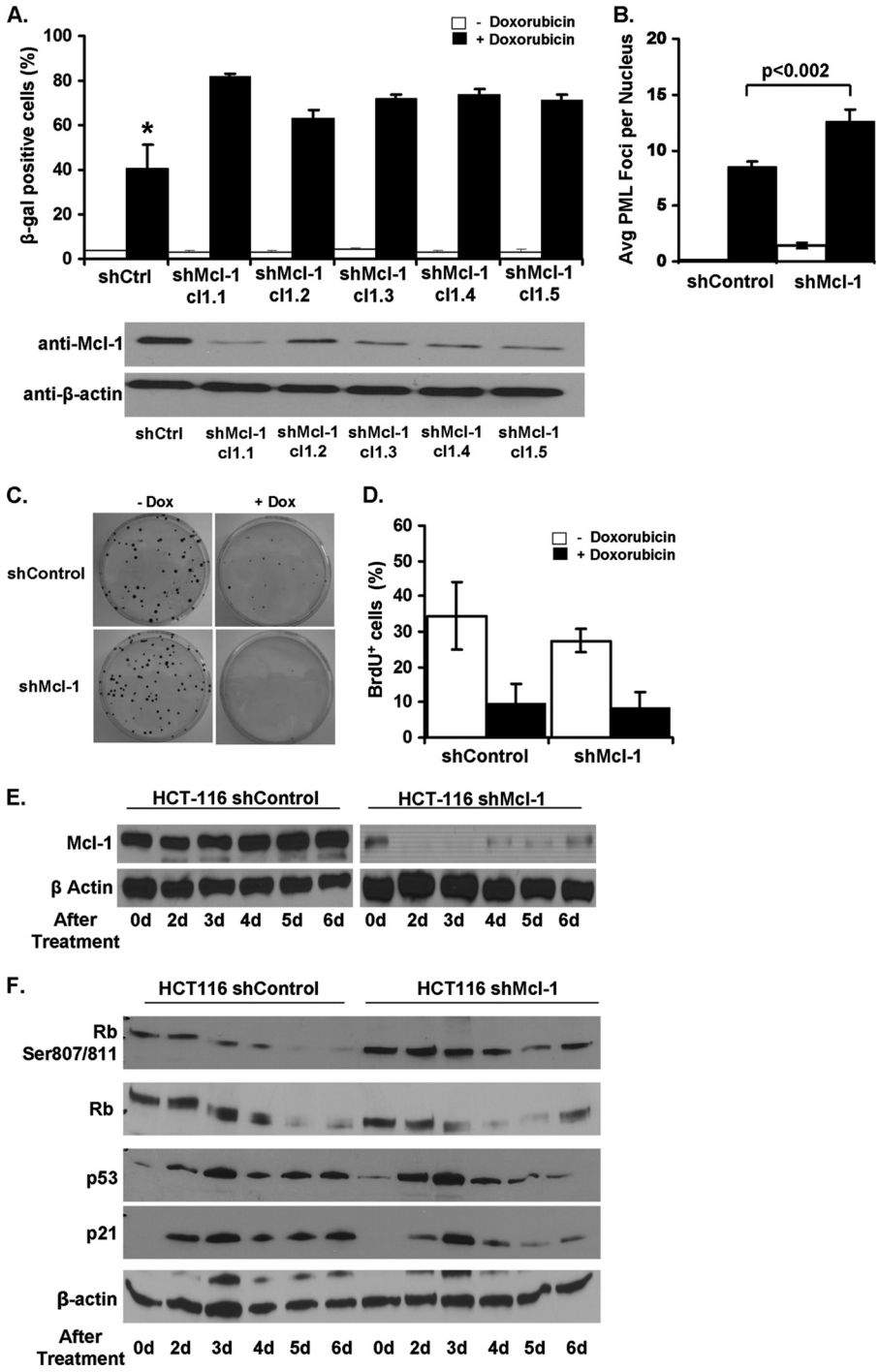


**FIG 2** Downregulation of Mcl-1 expression in HCT116 cells enhances CIS. (A) Percentages of SA-β-gal$^+$ HCT116 cells expressing shMcl-1 (or a nonspecific control) after 6 days of growth with or without 100 ng/ml doxorubicin (Dox). Represented on the graph are five independently generated shMcl-1 clones. Clone 1.1 (cl1.1) was used in subsequent experiments. Western blot analysis verifying Mcl-1 knockdown in each of the five shMcl-1 clones. (B) Average number of PML bodies per nucleus with or without doxorubicin for 4 days. Values represent the mean ± SD of at least three independent experiments. (C) Colony formation by HCT116 shControl and shMcl-1 cells growing with or without doxorubicin. (D) Quantification of BrdU incorporation. Values represent the mean ± SD of at least three independent experiments. (E) Western blot analysis of Mcl-1 protein expression in untreated cells (0 days) or 2, 3, 4, 5, and 6 days following doxorubicin treatment. (F) Western blot analysis of the indicated proteins in HCT116 shControl and shMcl-1 cells after doxorubicin treatment for 0, 2, 3, 4, 5, and 6 days.

sults in an increase in SA-β-gal$^+$ activity similar to HCT116 cells (Fig. 3H). Roscovitine suppresses Mcl-1 expression as previously reported (Fig. 3I) (24). Interestingly, the reduction of Mcl-1 was noticed as little as 2 h posttreatment and began to recover by 24 h. This observation suggests that downregulation of Mcl-1 is needed only for a few hours after chemotherapy treatment for initiating senescence. In summary, homeostatic levels of Mcl-1 seem to block a p53- and pRb-independent pathway of senescence, which

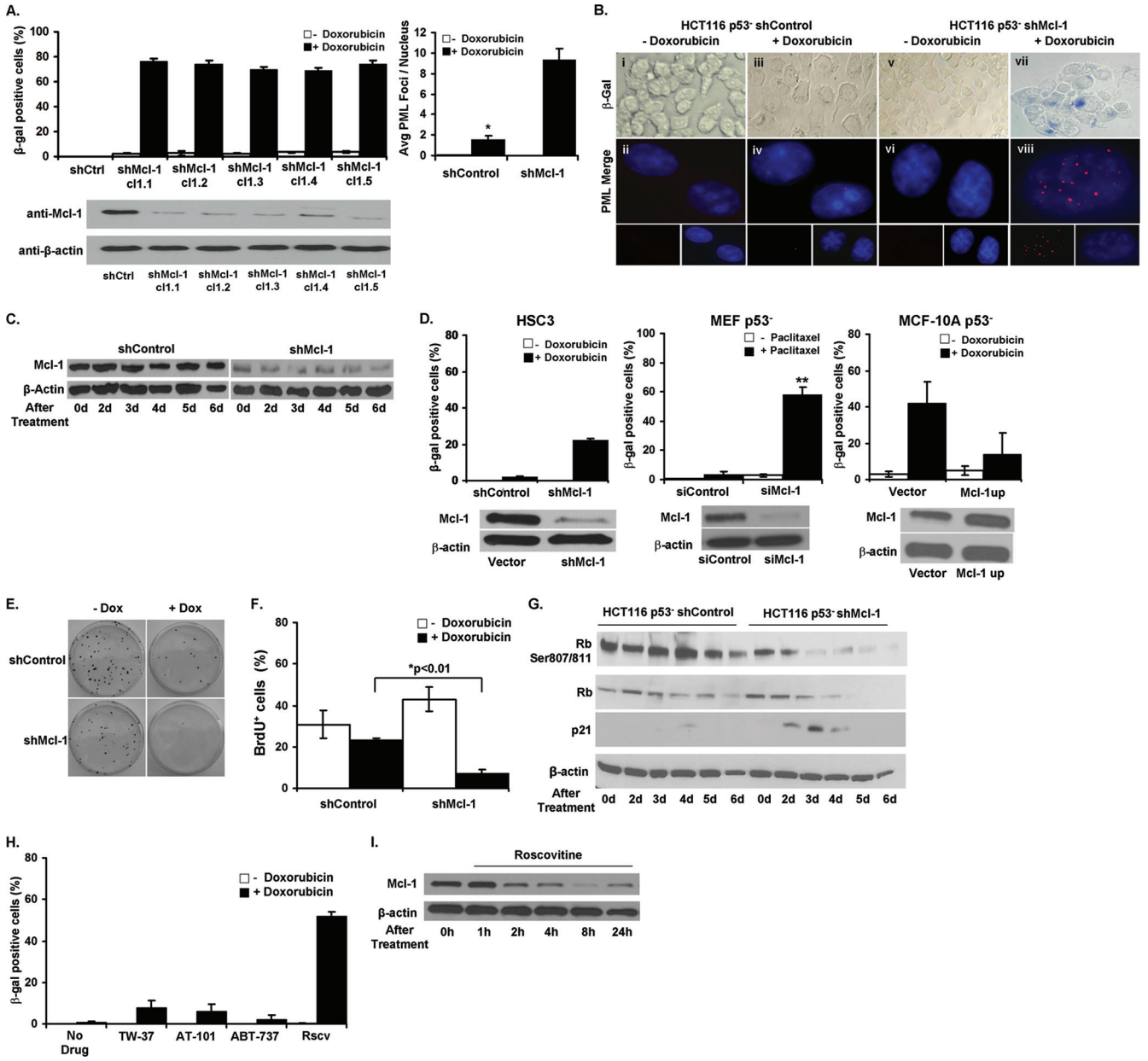


**FIG 3** Downregulation of Mcl-1 in HCT116 p53$^-$ cells allows for the induction of CIS. (A) Percentages of SA-β-gal$^+$ HCT116 p53$^-$ shControl and 5 shMcl-1 clones after 6 days of growth in media with or without doxorubicin (Dox). Clone 1.1 (cl1.1) was used in subsequent experiments. Western blot analysis of Mcl-1 expression in shControl or shMcl-1 clones after 6 days of treatment with doxorubicin. Average number of PML bodies per nucleus in HCT116 p53$^-$ cells with or without doxorubicin for 4 days. Values represent the mean ±SD of at least three independent experiments. (B) SA-β-gal$^+$ HCT116 p53$^-$ shControl and shMcl-1 cells after culture with or without 100 ng/ml doxorubicin for 6 days (panels i, iii, v, vii) (magnification, ×40). PML body staining (red) of HCT116 p53$^-$ vector and HCT116 Mcl-1up cells grown with or without doxorubicin for 6 days (panels ii, iv, vi, viii). Nuclei were counterstained with DAPI (magnification, ×100). Micrographs are representative of at least 3 independent experiments. (C) Western blot analysis of Mcl-1 expression in shControl or shMcl-1 cells left untreated (0 days) or 2, 3, 4, 5, and 6 days following doxorubicin treatment. (D) Percentages of SA-β-gal$^+$ cells among various p53$^-$ cell lines possessing altered Mcl-1 expression after 6 days treatment with either doxorubicin (HSC3 and MCF-10A) or paclitaxel (MEF). Values represent the mean ± SD of at least three independent experiments. **, *P* value of <0.001 for paclitaxel-treated siMcl-1 MEFs compared to treated siControl cells. Western blots indicating Mcl-1 expression in each cell line appear below each graph. (E) Colony formation by HCT116 p53$^-$ shControl and shMcl-1 cells growing in media with or without doxorubicin. (F) Quantification of BrdU incorporation. Values represent the mean ± SD of at least three independent experiments. *, *P* value of <0.01 for doxorubicin-treated shMcl-1 cells compared to treated shControl cells. (G) Western blot analysis of the expression of the indicated proteins in p53$^-$ shControl and shMcl-1 cells left untreated (0 days) or after 2, 3, 4, 5, and 6 days of treatment with doxorubicin. (H) Percentages of SA-β-gal$^+$ HCT116 p53$^-$ cells after 6 days growing in media with or without doxorubicin in combination with TW-37 (2 nM), AT-101 (2.5 μM), ABT-737 (10 μM), or roscovitine (Rscv) (25 μM). Values represent the mean ± SD of at least three independent experiments. (I) Western blot analysis of Mcl-1 expression after treatment with roscovitine for the indicated time points.

can be initiated via low-dose doxorubicin treatment in HCT116 p53$^-$ shMcl-1 cells.

**Mcl-1 has distinct antisenescent properties compared to other Bcl-2 family members.** We next wanted to determine whether other Bcl-2 family members play a similar role in CIS resistance. Using a specific shRNA (shBcl-2), we knocked down the Bcl-2 protein in HCT116 p53$^-$ cells. However, unlike Mcl-1, downregulation of Bcl-2 did not induce senescence following doxorubicin treatment (Fig. 4A). We also repeated these experiments using another Bcl-2-specific shRNA and obtained similar results (data not shown). It is interesting to note that overexpression of Bcl-2 alone can prevent chemotherapy-induced apoptosis but does not enhance colony formation (39). In contrast, as shown in Fig. 1D, overexpression of Mcl-1 did enhance colony formation in the presence of low-dose chemotherapy. These observations illustrate a distinct activity for Mcl-1 among Bcl-2 family members.

We next wanted to directly compare overexpression of Mcl-1 in p53$^-$ (Fig. 4B) and p53$^+$ (Fig. 4C) cells with other Bcl-2 family members (Bcl-2, Bcl-xL). We observe that all Bcl-2 family members tested have significant anti-CIS properties in p53$^+$ cells (Fig. 4C). In contrast, only overexpression of Mcl-1 significantly abrogates CIS in HCT116 p53$^-$ cells (Fig. 4B). These differences highlight a unique role for Mcl-1 in the regulation of a p53-independent senescence pathway.

We also employed another approach to inhibit Bcl-2 family members by using several small molecule inhibitors of Bcl-2 family proteins. ABT-737 (a BH3 mimetic) is designed to promote tumor cell apoptosis by blocking interaction between the prosurvival and proapoptotic (BH3-only) members of the Bcl-2 family. ABT-737 efficiently blocks Bcl-2 and Bcl-xL function but not Mcl-1 and on its own was shown to induce senescence in some but not all tumor cell lines (6, 30). Surprisingly, the fraction of SA-β-gal$^+$ cells was moderately reduced in HCT116 cells after treatment with ABT-737 and doxorubicin (Fig. 4D). This result may be explained by increased levels of Mcl-1 in ABT-737-treated cells (Fig. 4E). ABT-737 is known to cause the release of Bim, which can then stabilize and increase the expression of Mcl-1 protein (8). Additionally, we used a similar small molecule inhibitor, AT-101, which can block Bcl-2, Bcl-xL, and Mcl-1 in a similar fashion as ABT-737 (15). AT-101 did not affect the level of senescence induced by low-dose chemotherapy (Fig. 4D). We did confirm that the dose of AT-101 was sufficient to inhibit these antiapoptotic Bcl-2 family members and that AT-101 sensitized HCT116 cells to apoptosis after increasing doses of doxorubicin (data not shown). Using an additional small molecule inhibitor with similar properties as AT-101, TW-37, we also observed no increases in CIS (data not shown). We also tested all three small molecule inhibitors in HCT116 p53$^-$ cells, and none induced or sensitized the induction of senescence (Fig. 3H). These findings are important, as these inhibitors, which only target the binding site of BH3-only proapoptotic molecules, appear not to be involved in senescence promotion.

To further confirm that the antisenescent and antiapoptotic properties of Mcl-1 are unique, we obtained two well-described mutant versions of Mcl-1. First, we procured the recombinant Mcl-1ΔC protein lacking the final C terminus/transmembrane domain. This mutant has marginally reduced antiapoptotic function, because the C terminus is in part responsible for the targeting and retention of Mcl-1 to the mitochondria (10). A second mutant was obtained containing specific point mutations within the BH3 binding pocket that changes the binding specificity to BH3-only proteins and has significantly decreased antiapoptotic activity (13). Therefore, each of these mutants addressed the affect of its respective altered domain on senescence. Similar to normal Mcl-1, overexpression of both mutants protects against CIS in both p53$^-$ and p53$^+$ cells (Fig. 4B and C). These results indicate that the mechanism by which Mcl-1 inhibits senescence is neither dependent on its C-terminal transmembrane domain or its BH3 binding groove. These data, along with the results obtained using the small molecule inhibitors, indicate that a unique, still undefined area within Mcl-1 is responsible for its antisenescent function.

**CIS is dependent on p21.** We have shown that Mcl-1 can regulate both a p53-dependent and -independent senescence pathway. Previous work has demonstrated that HCT116 p21$^-$ cells also do not undergo senescence in the presence of low-dose chemotherapy (18). We next assessed whether Mcl-1 knockdown can restore senescence in these cells. As shown in Fig. 5A, downregulation of Mcl-1 either by shMcl-1 or by roscovitine did not induce senescence after treatment with low-dose doxorubicin. The downregulation of Mcl-1 in HCT116 p21$^-$ cells was confirmed by Western blotting (Fig. 5A, inset). Consistent with the lack of detectable senescence, we also did not observe any significant changes in p53 or pRb protein expression under these conditions (Fig. 5B). Thus, Mcl-1 loss, which appears to allow the induction of a p53-independent senescence pathway, did not affect HCT116 p21$^-$ cells, indicating that this pathway relies on p21.

Other studies have shown that p21 acts within the DNA damage response and ROS signaling pathway to induce senescence (20, 26). Therefore, we examined the kinetics of ROS production in HCT116 p53$^-$ cells left untreated, treated with doxorubicin, or treated with doxorubicin plus the antioxidant *N*-acetylcysteine (NAC). Inhibition of Mcl-1 in HCT116 p53$^-$ cells resulted in an increase in ROS production when treated with doxorubicin, which could be abrogated by the addition of NAC (Fig. 5C). Consistent with our observation that Mcl-1-mediated resistance to senescence is not related to the C terminus or BH3 binding pocket, the expression of our Mcl-1 mutants in HCT116 p53$^-$ shMcl-1 cells were just as effective at blocking ROS production as the reexpression of full-length Mcl-1 (Fig. 5C). HCT116 p53$^-$ shMcl-1 cells had greatly enhanced p21 expression within 24 h of doxorubicin treatment, which the addition of NAC blocked (Fig. 5D). These data suggest that Mcl-1 acts to suppress ROS production, thereby inhibiting the expression of p21. Further, there was a decrease in SA-β-gal$^+$ cells when HCT116 p53$^-$ shMcl-1 cells were treated with doxorubicin plus NAC (Fig. 5E). Thus, we demonstrate that Mcl-1 can suppress ROS production in HCT116 p53$^-$ cells, thereby inhibiting p21 expression and ultimately CIS.

**Mcl-1 controls tumor growth *in vivo*.** To evaluate CIS *in vivo*, we injected various HCT116 cell lines (HCT116 Mcl-1up, HCT116 vector, HCT116 p53$^-$ shMcl-1, HCT116 p53$^-$ shControl) into athymic nude mice. Untreated control tumors of both HCT116 and HCT116 p53$^-$ cell lines displayed robust growth (Fig. 6A). However, downregulation of Mcl-1 (shMcl-1) in both HCT116 and HCT116 p53$^-$ cell lines severely inhibited tumor growth. Enhanced SA-β-gal$^+$ activity was observed in both HCT116 and HCT116 p53$^-$ shMcl-1 tumors as well as a reduction in Ki-67 expression (Fig. 6B and C). We additionally confirmed persistent Mcl-1 downregulation *in vivo* in all shMcl-1 tumors and found

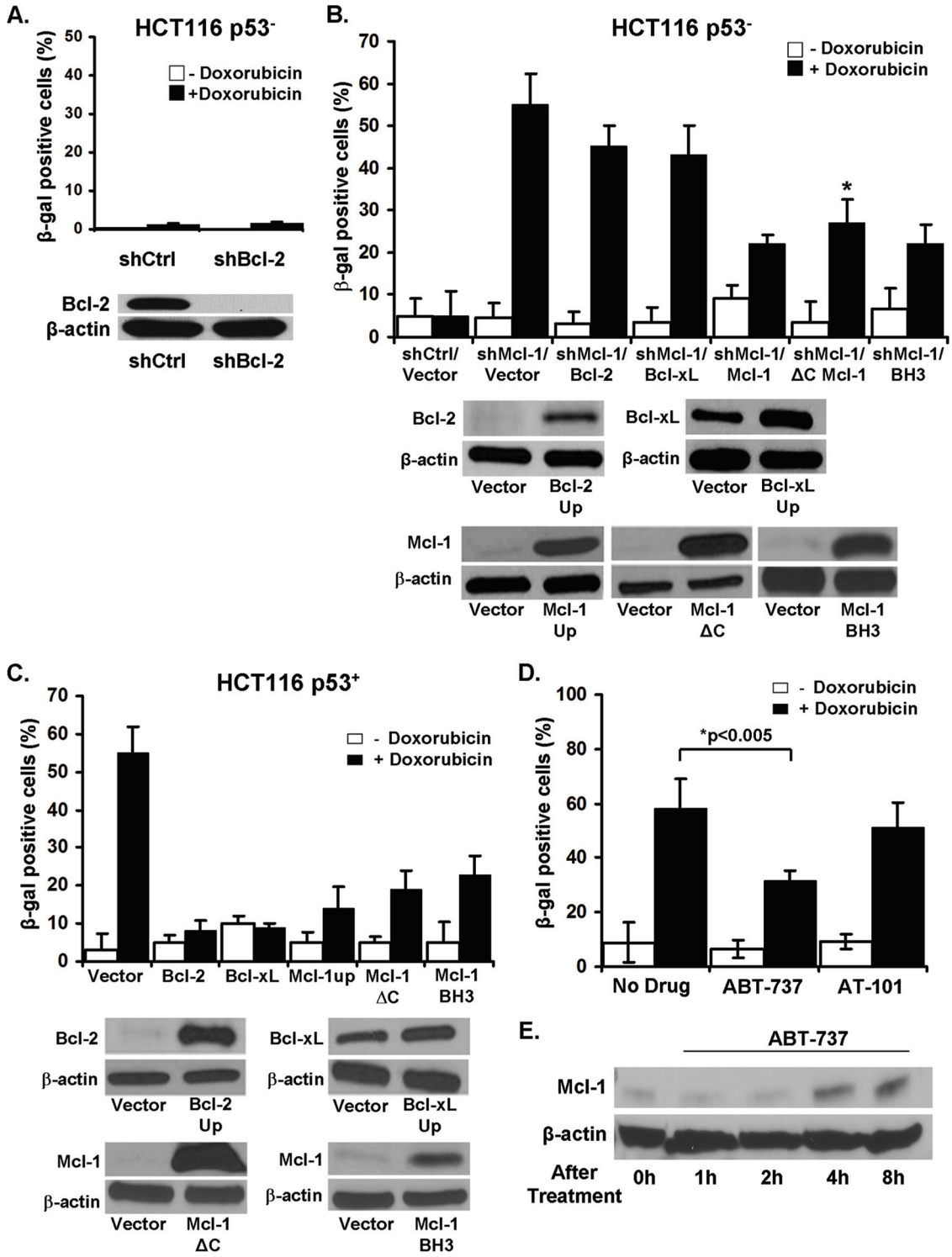


**FIG 4** Mcl-1 is unique among Bcl-2 family members in its ability to induce senescence in p53$^{-}$ cells. (A) Percentages of SA-β-gal$^{+}$ HCT116 p53$^{-}$ cells expressing a shRNA specific for Bcl-2 or an irrelevant control after 6 days culture with or without doxorubicin. Western blot verification of the knockdown of Bcl-2 expression. (B) Percentages of SA-β-gal$^{+}$ HCT116 p53$^{-}$ shControl cell line or HCT116 p53$^{-}$ shMcl-1 cell line plus vector control, overexpressing exogenous Bcl-2, Bcl-xL, Mcl-1, Mcl-1 with a deleted C-terminal/transmembrane mitochondrial targeting domain (Mcl-1ΔC), and Mcl-1 with a mutated BH3 binding groove (BH3) grown for 6 days with or without doxorubicin. Values represent the mean ± SD of at least three independent experiments. Western blot verification of exogenous gene expression in each cell line. (C) Percentages of SA-β-gal$^{+}$ HCT116 p53$^{+}$ cells with control vector or overexpressing exogenous Bcl-2, Bcl-xL, Mcl-1, Mcl-1ΔC, or BH3 mutant Mcl-1 grown in media for 6 days with or without doxorubicin. No significant differences were observed between normal Mcl-1 overexpression and the two mutant versions of the Mcl-1 molecule. Values represent the mean ± SD of at least three independent experiments. Western blot verification of protein overexpression in each cell line. (D) Percentages of SA-β-gal$^{+}$ HCT116 cells after 6 days of growth in media alone or with ABT-737 or AT-101 and with or without doxorubicin. Values represent the mean ± SD of at least three independent experiments. (E) Western blot analysis of Mcl-1 expression after treatment with ABT-737 for the indicated time points.

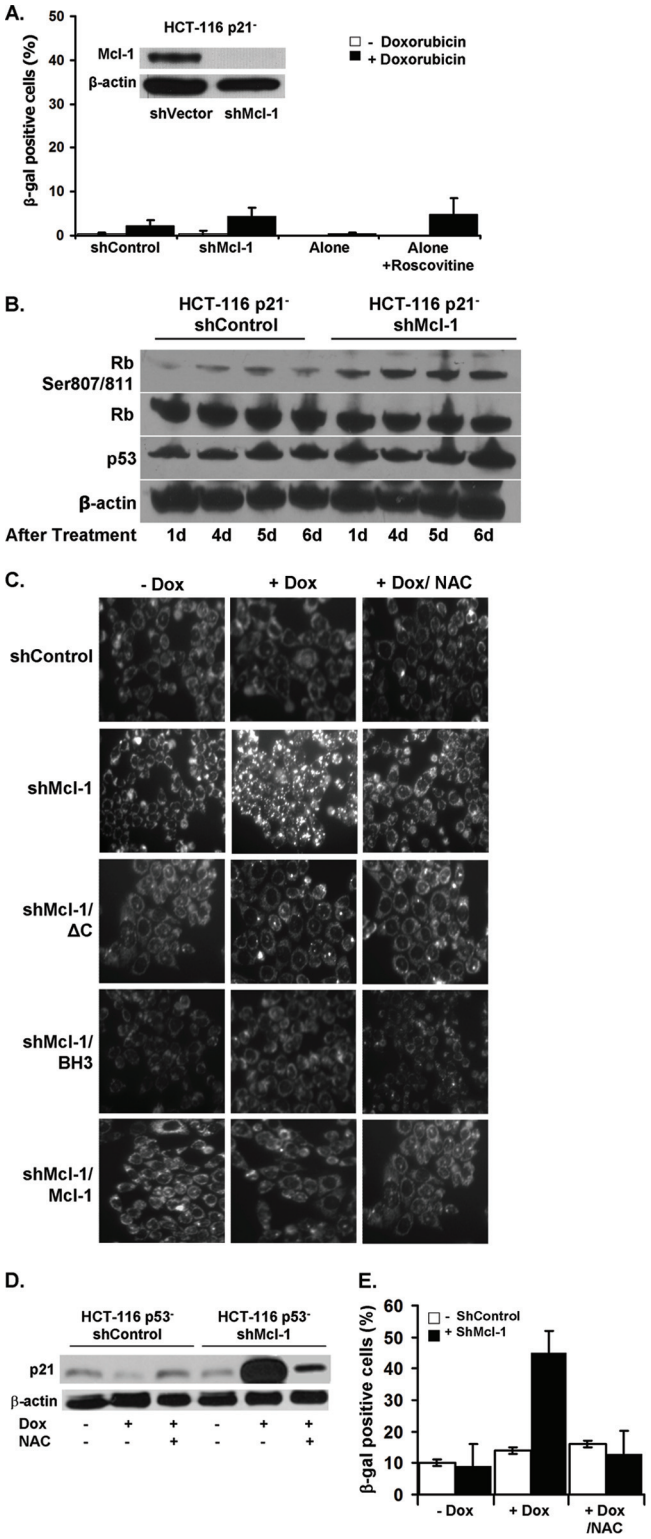


**FIG 5** Senescence induction in p53$^-$ cells requires p21 induction via a pathway involving reactive oxygen species (ROS) production. (A) The percentages of SA-β-gal$^+$ HCT116 p21$^-$ cells expressing shControl, shMcl-1, alone, or treated with roscovitine after 6 days of culture in media with or without doxorubicin (Dox). (Inset) Western blot verifying knockdown of Mcl-1 in HCT116 p21$^-$ cells. (B) Western blot analysis of the indicated proteins in HCT116 p21$^-$ shControl or shMcl-1 cells at the indicated days after treatment with doxorubicin. (C) HCT116 p53$^-$ shControl or shMcl-1 cells alone or also expressing exogenous Mcl-1ΔC, Mcl-1 BH3 mutant, or Mcl-1 were pretreated with 5 μM NAC for 24 h followed by doxorubicin treatment for 6 days (magnification, ×20). Cells were then stained with RedoxSensor Red to visualize ROS production. (D) Cells were pretreated with NAC or left untreated for 24 h, followed by treatment with doxorubicin. After 6 days of treatment, lysates were prepared and assayed for p21 expression by Western blotting. (E) The percentages of SA-β-gal$^+$ HCT116 p53$^-$ cells after 6 days of culture with or without doxorubicin in NAC pretreated or untreated cells.

little apoptosis in all tumors via TUNEL staining (Fig. 6B). These observations illustrate that forced reduction of Mcl-1 expression retards tumor growth even in HCT116 p53$^-$ cells, and this growth reduction is associated with senescence.

**Inhibition of ROS production restores growth of p53$^-$ shMcl-1 tumors.** Because the production of ROS was found to play a key role in senescence induction in p53$^-$ HCT116 cells *in vitro*, we next determined whether it could also block senescence *in vivo*. Previous reports found that NAC treatment of p53$^-$ xenograft tumors could result in a delay in tumor growth, mostly likely due to the inhibition of ROS-related DNA damage and genomic instability (27). Using a similar treatment regimen in which tumor-bearing mice received oral NAC, we observed that the growth of HCT116 p53$^-$ tumors possessing normal Mcl-1 expression could be slightly delayed. In contrast, the growth inhibition caused by knockdown of Mcl-1 expression could be almost completely abrogated by NAC treatment (Fig. 7A). NAC-treated p53$^-$ shMcl-1 tumors had reduced SA-β-gal activity and greater Ki-67 expression compared to the untreated shMcl-1 group (Fig. 7B and C). All tumor groups had similar low levels of apoptosis as measured by TUNEL staining. Tumor outgrowth was not due to the loss of Mcl-1 knockdown, as treated and untreated tumors had similarly reduced levels of Mcl-1 expression. Further, the enhanced tumor growth caused by ROS inhibition appears to be specific to the p53-independent senescence pathway, as NAC treatment of p53$^+$ control and shMcl-1 tumors had no observable effect on tumor growth (data not shown). Collectively, these data underscore the key role ROS production plays in p53-independent senescence pathways and the importance of Mcl-1 in their inhibition.

**Mcl-1 prevents doxorubicin-induced cellular senescence *in vivo*.** In order to determine if overexpression of Mcl-1 can prevent senescence induced by a low dose of doxorubicin *in vivo*, HCT116 tumor cells overexpressing Mcl-1 or an empty vector were transplanted into nude mice and then, after 10 days, treated with 1.2 mg/kg doxorubicin once every third day. This dose of doxorubicin was chosen based on previous reports (38). Doxorubicin effectively inhibited growth and induced SA-β-gal$^+$ activity in tumors expressing empty vector (Fig. 8A and B). Similarly, the percentage of cells expressing Ki-67 was significantly lower in doxorubicin-treated tumors expressing empty vector (Fig. 8C). In contrast, tumors overexpressing Mcl-1 grew robustly despite doxorubicin treatment and were, from a growth curve standpoint, almost resistant to treatment (Fig. 8A). We also did not observe any reduction of Ki-67 staining in drug-treated Mcl-1 overexpressing tumors (Fig. 8C). Our data show that overexpression of Mcl-1 in HCT116 cells promotes tumor growth *in vivo* and creates resistance to chemotherapy treatment and its resultant induction of senescence.

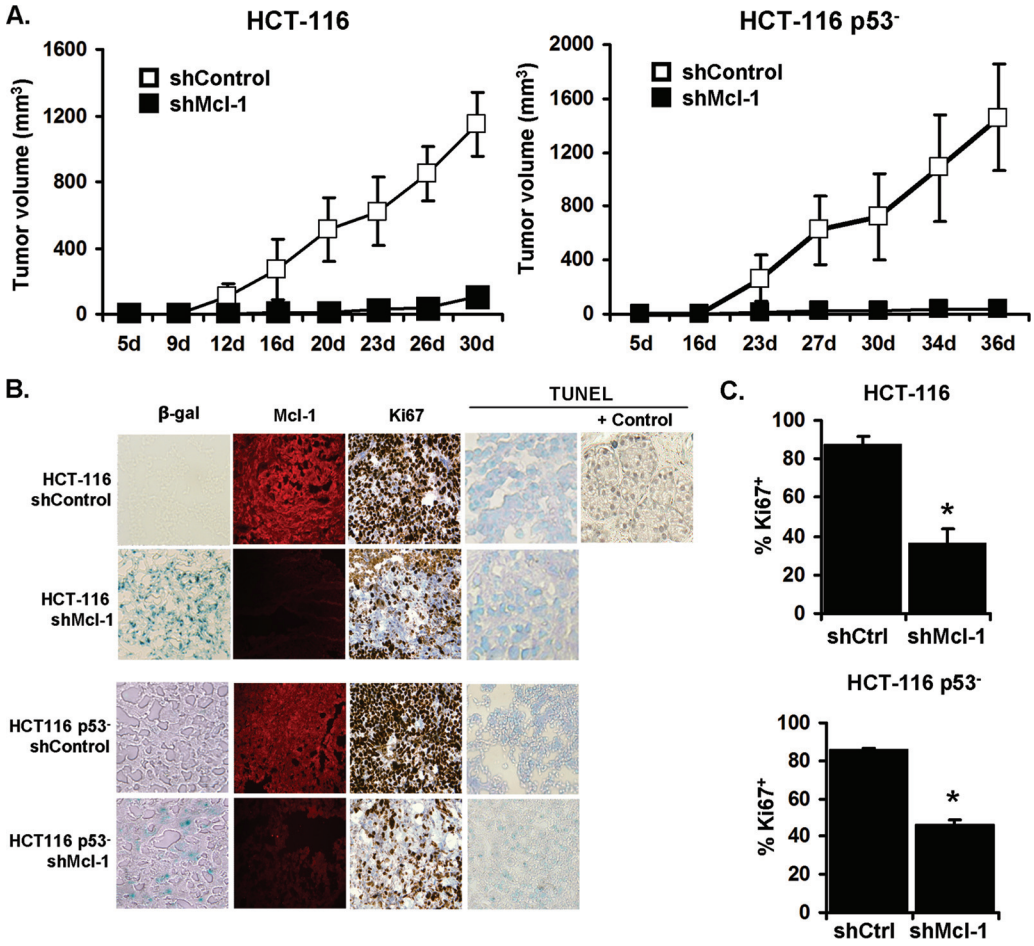


**FIG 6** Downregulation of Mcl-1 in HCT116 and HCT116 p53$^-$ induces senescence *in vivo*. (A) Growth curves of HCT116 shControl and shMcl-1 in athymic nude mice. A total of $1 \times 10^7$ cells were injected subcutaneously into the right dorsal flank ($n = 5$). Data points are mean ± SD values of tumor volumes. (B) Immunohistology of HCT116 shControl and shMcl-1 xenograft tumors, staining for Mcl-1, Ki-67, and TUNEL analysis were done using formalin-fixed and frozen sections. (C) The percentage of Ki-67$^+$ cells in the indicated tumor sections. Data are presented as mean ± SD. *, *P* value of $<0.05$ for Ki-67 expression in shMcl-1 cells compared to shControl. Data are indicative of three replicate experiments.

## DISCUSSION

Senescence is a recognized cellular pathway involved in all aspects of cancer biology from carcinogenesis to tumor proliferation and treatment sequela and appears to be a major hurdle for cancer progression (14). Senescence appears to be controlled by distinct pathways but, in general, is initiated by tumor suppressors like p53. Interestingly, various oncogenes induce senescence, a response which appears to be the major barrier to the development of cancer (35). Thus, without evasion or loss of tumor suppressor genes such as p53, cells expressing or even overexpressing oncogenes fail to become cancerous due to senescence (2). In the realm of cancer therapy, apoptosis has been the main form of cell death studied in response to chemotherapy and radiation therapy (25). However, recent studies have described how similar treatments of p53$^-$ cells in which p53 expression was restored resulted in tumor regression through the induction of senescence (34, 37). Further, chemotherapies have been reported to induce senescence in a variety of cancer types in human patients, which is associated with treatment success (14). In this regard, tumor senescence escape mechanisms not only have implications in carcinogenesis but treatment efficacy as well.

Our study reveals that a well-known antiapoptotic gene, Mcl-1, which is overexpressed in many cancers and has been studied mainly in hematopoietic malignancies, protects several solid cancer cell lines from CIS (10, 30, 39). Mcl-1's homeostatic and antiapoptotic properties have been well described (28, 39); however, its senescence-modulating functions have not been studied until this report. The antisenescent function of Mcl-1 appears to be distinct from its related Bcl-2 family members. For instance, Bcl-2 was reported to be unable to inhibit senescence (29). The differences between these related molecules is further underscored by the finding that, in complementary mouse models of leukemia, tumor cells dependent on Mcl-1 were more susceptible to chemotherapy than those dependent on Bcl-2 (5). Our data reveal that all major Bcl-2 antiapoptotic molecules (Mcl-1, Bcl-2, and Bcl-xL) are antisenescent in p53$^+$ tumors; however, there appears to be a distinct ability of Mcl-1 to inhibit CIS in p53$^-$ cells. These differences underscore the uniqueness of the p53$^-$ pathway to senescence and highlight the need for its further characterization.

During the process of senescence induction we observe, in both p53$^+$ and p53$^-$ cells, induction and dependence on p21 as well as

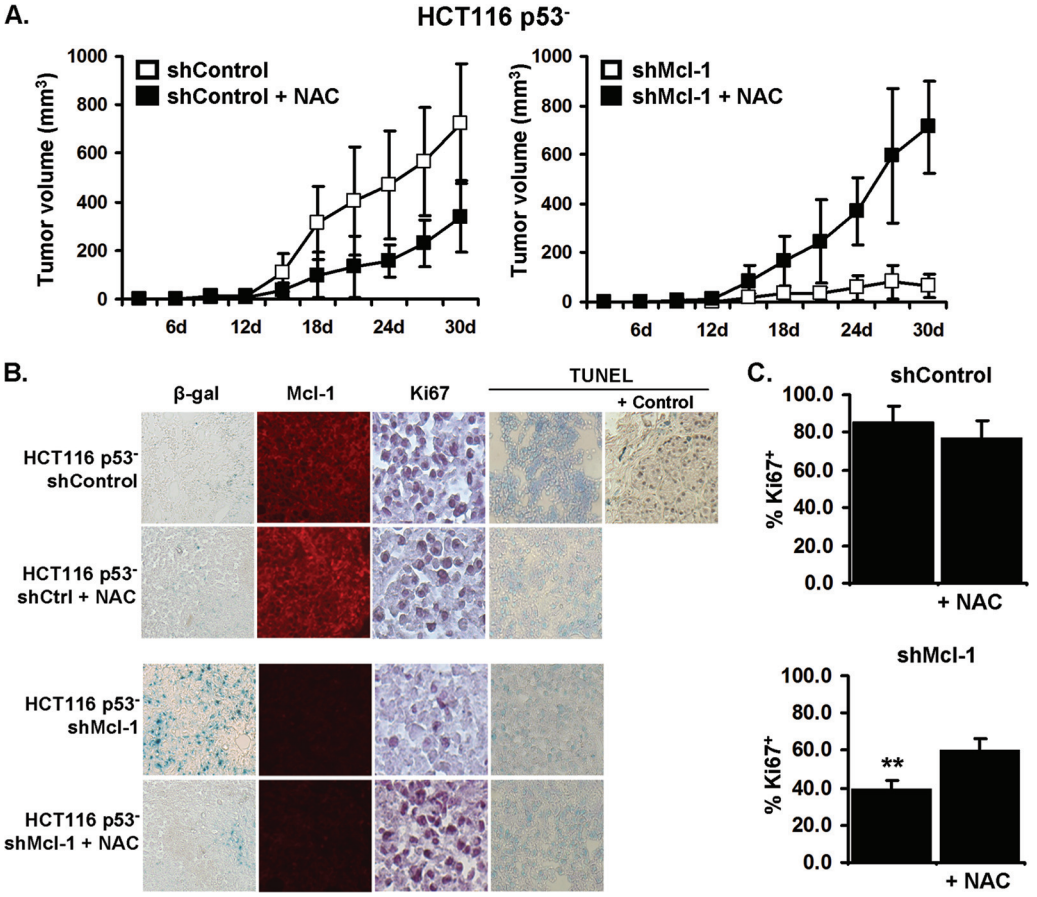


**FIG 7** Antioxidant treatment of HCT116 p53$^-$ shMcl-1 tumors *in vivo* can enhance tumor growth. (A) Growth curves of HCT116 p53$^-$ shControl and shMcl-1 tumors implanted in athymic nude mice. A total of $1 \times 10^7$ cells were injected subcutaneously into the right dorsal flank ($n = 5$). *N*-Acetylcysteine (NAC) treatment groups received drinking water containing 40 mM NAC. Marked are mean ± SD values of tumor volumes. (B) Immunohistology of indicated tumors after growth in nude mice. SA-β-gal, Mcl-1, Ki-67, and TUNEL staining was performed on formalin-fixed and frozen sections. (C) The percentage of Ki-67$^+$ cells in tumor sections. Data are presented as mean ± SD. **, *P* value of <0.001 in NAC-treated shMcl-1 tumors compared to untreated shMcl-1. Data are indicative of three replicate experiments.

a loss of pRb. These findings agree with a similar study of doxorubicin- and radiation-induced senescence in p53$^+$ cells, which also required p21 induction and was accompanied by pRb loss (19). This study further found a role for another pocket protein, Rb2, which was strongly upregulated during senescence. Another recent study described how loss of pRb was a senescence escape mechanism in normal human fibroblasts (9). That study further showed that pRb loss triggered an additional proliferation barrier via p21-driven induction of senescence. Based on these studies, we hypothesize that loss of pRb expression in our model may be part of a p21-dependent progression into senescence.

Senescence pathways independent of p53 have been described but are still poorly understood (20). Our results reveal that in p53$^-$ cells (which do not normally undergo CIS), chemotherapy treatment can induce senescence after knockdown of Mcl-1 expression. This process causes similar changes to those found in p53$^+$ cells, including increases in p21 expression, loss of pRb, enhanced PML body formation, and reduced BrdU incorporation. This implies that homeostatic levels of Mcl-1 govern an alternate pathway which is not dominant when p53 is active.

Similar experiments in HCT116 p21$^-$ cells reveal that p21 is indispensable for senescence induction even when Mcl-1 is knocked down. Others have shown that p21 expression during senescence is dependent on the production of ROS (26, 36). We observe that in the absence of p53, not only does knockdown of Mcl-1 expression result in enhanced ROS production concomitant with SA-β-gal activity after doxorubicin treatment, but the addition of an antioxidant is sufficient to block the induction of both ROS and senescence. This observation is further underscored by the use of NAC to block ROS production *in vivo*. Whereas we and others have demonstrated the ability of NAC treatment to slow the growth of p53$^-$ tumors, we find that NAC can accelerate the growth of p53$^-$ tumors also lacking Mcl-1, suggesting that NAC's ability to inhibit senescence and thus promote tumor growth is stronger than the protective effects of preventing ROS-related DNA damage in these cells (27). Collectively, these results imply that in p53$^-$ cells, Mcl-1 acts to prevent ROS induction perhaps in a manner similar to that reported for Bcl-2 in p53$^+$ cells and that chemotherapy induces senescence primarily through a p53/p21 axis, but without p53, the loss of Mcl-1 can activate an alternative pathway to senescence that is ROS and p21 dependent (21). The trigger for this pathway is still under investigation but we hypothesize that other tumor suppressors are involved (8).

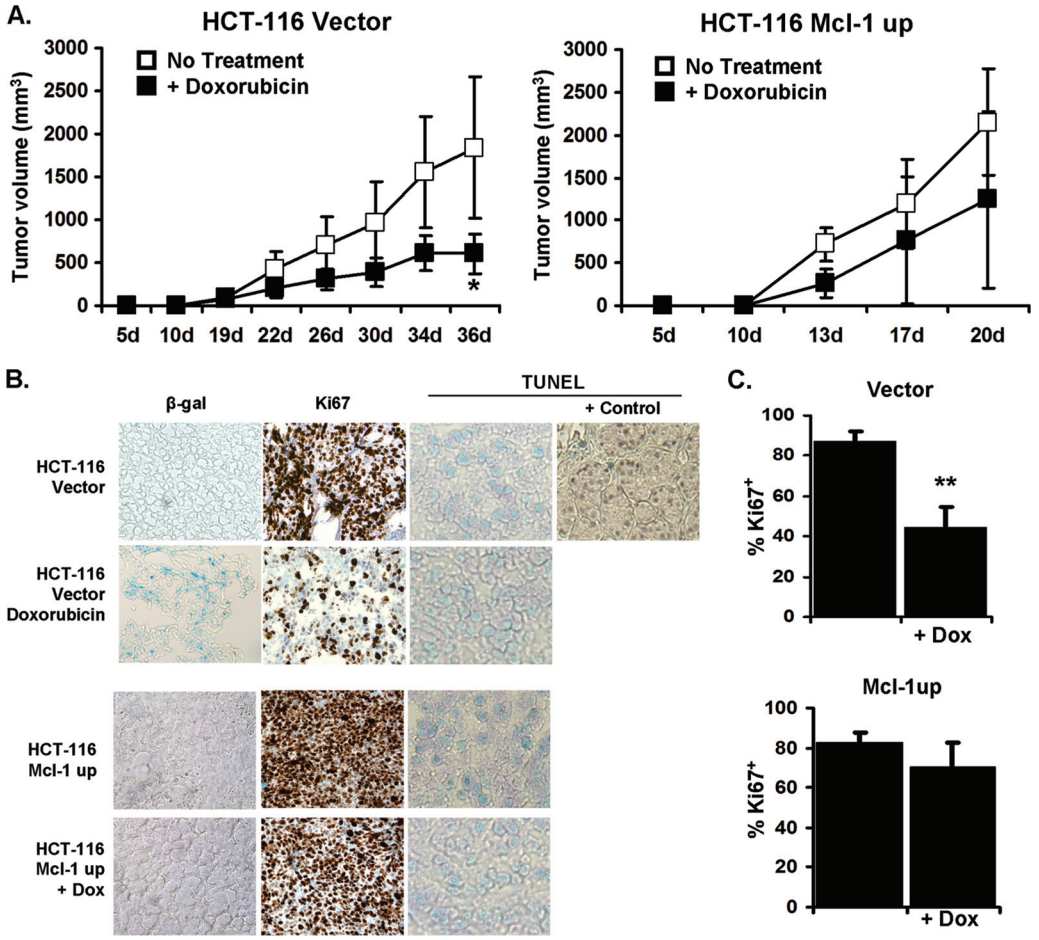


**FIG 8** Overexpression of Mcl-1 in HCT116 prevents CIS in xenograft tumor-bearing nude mice. (A) Growth curves of HCT116 vector control or Mcl-1 overexpressing tumors in nude mice. A total of $1 \times 10^7$ cells were injected into the right dorsal flank of female mice, and after 10 days, the animals were distributed into groups receiving PBS alone (no treatment) or 1.2 mg/kg of doxorubicin (Dox) in PBS every third day intraperitoneally ($n = 5$). Data points are mean ± SD values of tumor volumes. *, $P$ value of $<0.05$ between doxorubicin-treated and untreated groups. (B) Immunohistology of HCT116 vector and Mcl-1up tumors. SA-β-gal, Ki-67, and TUNEL staining were done using formalin-fixed and frozen sections. (C) The percentage of $Ki67^+$ cells was determined in the indicated tumor sections. Data are presented as mean ± SD. **, $P$ value of $<0.001$ between the doxorubicin-treated and untreated vector control tumors. Data are representative of three independent studies.

In order to determine whether the canonical BH3 binding domain of Mcl-1 is involved in resisting the induction of CIS as it is for apoptosis, we blocked interaction with this domain through the use of small molecule inhibitors. BH3 mimetics are in various levels of preclinical and clinical trials and block the interaction between antiapoptotic Bcl-2 molecules and their proapoptotic counterparts, leaving the latter molecule free to induce apoptosis (15). We show for the first time that a gossypol variant, AT-101, which targets most major antiapoptotic Bcl-2 family members, including Mcl-1, did not alter the level of CIS. Interestingly, another BH3 mimetic, ABT-737, which does not target Mcl-1, failed to increase senescence and actually partially decreased it. We subsequently found that ABT-737 increases Mcl-1 expression, likely due to its anti-Bcl-2/Bcl-xL effects, and this would explain the decreased senescence observed in ABT-737-treated cells (33). Similarly, other studies of ABT-737 reveal its inability to induce apoptosis in cells overexpressing or selected to overexpress Mcl-1 (38). Taken together, these data demonstrate that BH3 mimetics do not increase the level of CIS, thus indicating that the BH3 binding domain of Mcl-1 (or other Bcl-2 family members) is not involved in regulating CIS.

In order to conclusively exclude the BH3 binding domain of Mcl-1 from its antisenescent activity, we obtained an Mcl-1 mutant containing an inactive BH3 binding pocket (22). While this mutant possesses severely reduced antiapoptotic activity, we found that it nonetheless confers resistance to CIS similar to wild-type Mcl-1. We also obtained an Mcl-1 mutant containing a deletion of the C-terminal transmembrane/mitochondrial targeting domain, which was reported to have moderately reduced antiapoptotic activity, and likewise found that the deletion had minimal effect on its antisenescent properties (23). These data imply that Mcl-1-mediated inhibition of senescence is distinct from its antiapoptotic function and is not reliant on its ability to bind to BH3 proapoptotic molecules. Further, these data indicate that a distinct domain of the Mcl-1 molecule is responsible for its antisenescent function. Identifying this location within Mcl-1 will be the basis of further drug discovery.

Our results also indicate that human solid cancer cells require

Mcl-1 for tumor growth *in vivo* even in the absence of p53. These data are striking since loss of p53 is sufficient to initiate not only tumorigenesis but also cancer progression (34). Our data suggest that, from a tumor growth retardation standpoint, an Mcl-1-dependent and p53-independent process is dominant. Moreover, reduced levels of Mcl-1 even without any treatment were associated with senescence as indicated by SA-β-gal activity and abrogation of Ki-67 expression. When we examined CIS *in vivo*, we consistently observed that overexpression of Mcl-1 enhanced not only tumor growth but also resistance to CIS, suggesting that tumors which overexpress Mcl-1 basally or by selection are resistant to cancer treatment by resisting both apoptosis and senescence.

The implications of this study are that targeting Mcl-1 in cancers that either express this molecule or could be selected to express it may be an important aspect of cancer therapy. Further, molecular targeting could also be too specific in that "inhibitors" of a molecule may target only one aspect of its function. In the case of Mcl-1, small molecule inhibitors of apoptosis-associated domains are available; however, our study demonstrates that Mcl-1 also inhibits CIS via an undefined domain for which there is no specific inhibitor currently available. Future studies are required to develop complete inhibitors of Mcl-1 and similar molecules in order to target all of their cancer-promoting and treatment-resistant functions.

## ACKNOWLEDGMENTS

This work was supported by NIH grants R01CA132796 (to B.R.G.) and CA105005 (to D.V.K.).

## REFERENCES


1. **Bartkova J, et al.** 2006. Oncogene-induced senescence is part of the tumorigenesis barrier imposed by DNA damage checkpoints. Nature **444**: 633–637.
2. **Beauséjour CM, et al.** 2003. Reversal of human cellular senescence: roles of the p53 and p16 pathways. EMBO J. **22**:4212–4222.
3. **Beroukhim, R, et al.** 2010. The landscape of somatic copy-number alteration across human cancers. Nature **463**:899–905.
4. **Braig M, et al.** 2005. Oncogene-induced senescence as an initial barrier in lymphoma development. Nature **436**:660–665.
5. **Brunelle JK, Ryan J, Yecies D, Opferman JT, Letai A.** 2009. MCL-1-dependent leukemia cells are more sensitive to chemotherapy than BCL-2-dependent counterparts. J. Cell Biol. **187**:429–442.
6. **Bunz F, et al.** 1998. Requirement for p53 and p21 to sustain G2 arrest after DNA damage. Science **282**:1497–1501.
7. **Campisi J.** 2005. Senescent cells, tumor suppression, and organismal aging: good citizens, bad neighbors. Cell **120**:513–522.
8. **Chen Z, et al.** 2005. Crucial role of p53-dependent cellular senescence in suppression of Pten-deficient tumorigenesis. Nature **436**:725–730.
9. **Chicas A, et al.** 2010. Dissecting the unique role of the retinoblastoma tumor suppressor during cellular senescence. Cancer Cell **17**:376–387.
10. **Chipuk JE, et al.** 2008. Mechanism of apoptosis induction by inhibition of the anti-apoptotic BCL-2 proteins. Proc. Natl. Acad. Sci. U. S. A. **105**: 20327–20332.
11. **Chipuk JE, et al.** 2004. Direct activation of Bax by p53 mediates mitochondrial membrane permeabilization and apoptosis. Science **303**:1010–1014.
12. **Cichowski K, Hahn WC.** 2008. Unexpected pieces to the senescence puzzle. Cell **133**:958–961.
13. **Clohessy JG, Zhuang J, de Boer J, Gil-Gomez G, Brady HJ.** 2006. Mcl-1 interacts with truncated Bid and inhibits its induction of cytochrome c release and its role in receptor-mediated apoptosis. J. Biol. Chem. **281**: 5750–5759.
14. **Collado M, Serrano M.** 2010. Senescence in tumours: evidence from mice and humans. Nat. Rev. Cancer **10**:51–57.
15. **Gao P, et al.** 2010. The Bcl-2 homology domain 3 mimetic gossypol induces both Beclin 1-dependent and Beclin 1-independent cytoprotective autophagy in cancer cells. J. Biol. Chem. **285**:25570–25581.
16. **Halazonetis TD, Gorgoulis VG, Bartek J.** 2008. An oncogene-induced DNA damage model for cancer development. Science **319**:1352–1355.
17. **Han J, Goldstein LA, Gastman BR, Rabinowich H.** 2006. Interrelated roles for Mcl-1 and BIM in regulation of TRAIL-mediated mitochondrial apoptosis. J. Biol. Chem. **281**:10153–10163.
18. **Han J, Goldstein LA, Hou W, Gastman BR, Rabinowich H.** 2010. Regulation of mitochondrial apoptotic events by p53-mediated disruption of complexes between antiapoptotic Bcl-2 members and Bim. J. Biol. Chem. **285**:22473–22483.
19. **Helmbold H, Komm N, Deppert W, Bohn W.** 2009. Rb2/p130 is the dominating pocket protein in the p53-p21 DNA damage response pathway leading to senescence. Oncogene **28**:3456–3467.
20. **Inoue T, et al.** 2009. Level of reactive oxygen species induced by p21Waf1/CIP1 is critical for the determination of cell fate. Cancer Sci. **100**:1275–1283.
21. **Jung MS, et al.** 2004. Bcl-xL and E1B-19K proteins inhibit p53-induced irreversible growth arrest and senescence by preventing reactive oxygen species-dependent p38 activation. J. Biol. Chem. **279**:17765–17771.
22. **Konopleva M, et al.** 2006. Mechanisms of apoptosis sensitivity and resistance to the BH3 mimetic ABT-737 in acute myeloid leukemia. Cancer Cell **10**:375–388.
23. **Kuilman T, et al.** 2008. Oncogene-induced senescence relayed by an interleukin-dependent inflammatory network. Cell **133**:1019–1031.
24. **Leitch AE, et al.** 2010. The cyclin-dependent kinase inhibitor R-roscovitine down-regulates Mcl-1 to override pro-inflammatory signalling and drive neutrophil apoptosis. Eur. J. Immunol. **40**:1127–1138.
25. **Letai AG.** 2008. Diagnosing and exploiting cancer's addiction to blocks in apoptosis. Nat. Rev. Cancer **8**:121–132.
26. **Passos JF, et al.** 2010. Feedback between p21 and reactive oxygen production is necessary for cell senescence. Mol. Syst. Biol. **6**:347.
27. **Sablina AA, et al.** 2005. The antioxidant function of the p53 tumor suppressor. Nat. Med. **11**:1306–1313.
28. **Salomoni P, Pandolfi PP.** 2002. The role of PML in tumor suppression. Cell **108**:165–170.
29. **Schmitt CA, et al.** 2002. A senescence program controlled by p53 and p16INK4a contributes to the outcome of cancer therapy. Cell **109**:335–346.
30. **Song JH, Kandasamy K, Zemskova M, Lin YW, Kraft AS.** 2011. The BH3 mimetic ABT-737 induces cancer cell senescence. Cancer Res. **71**: 506–515.
31. **Soule HD, et al.** 1990. Isolation and characterization of a spontaneously immortalized human breast epithelial cell line, MCF-10. Cancer Res. **50**: 6075–6086.
32. **Tremml G, Singer M, Malavarca R.** 2008. Culture of mouse embryonic stem cells. Curr. Protoc. Stem Cell Biol. **1**:Unit 1C.4.
33. **van Delft MF, et al.** 2006. The BH3 mimetic ABT-737 targets selective Bcl-2 proteins and efficiently induces apoptosis via Bak/Bax if Mcl-1 is neutralized. Cancer Cell **10**:389–399.
34. **Ventura A, et al.** 2007. Restoration of p53 function leads to tumour regression in vivo. Nature **445**:661–665.
35. **Weiss MB, et al.** 2010. Deletion of p53 in human mammary epithelial cells causes chromosomal instability and altered therapeutic response. Oncogene **29**:4715–4724.
36. **Weyemi U, et al.** 15 August 2011. ROS-generating NADPH oxidase NOX4 is a critical mediator in oncogenic H-Ras-induced DNA damage and subsequent senescence. Oncogene. doi:10.1038/onc.2011.327.
37. **Xue W, et al.** 2007. Senescence and tumour clearance is triggered by p53 restoration in murine liver carcinomas. Nature **445**:656–660.
38. **Yecies D, Carlson NE, Deng J, Letai A.** 2010. Acquired resistance to ABT-737 in lymphoma cells that up-regulate MCL-1 and BFL-1. Blood **115**:3304–3313.
39. **Yin DX, Schimke RT.** 1995. BCL-2 expression delays drug-induced apoptosis but does not increase clonogenic survival after drug treatment in HeLa cells. Cancer Res. **55**:4922–4928.
40. **Zhou P, et al.** 2001. MCL1 transgenic mice exhibit a high incidence of B-cell lymphoma manifested as a spectrum of histologic subtypes. Blood **97**:3902–3909.